ACS APPLIED POLYMER MATERIALS

pubs.acs.org/acsapm Article

# Reactive Extrusion of Poly(lactic acid)-*graft*-Curcumin Antioxidant and Intelligent Packaging

Halle N. Redfearn and Julie M. Goddard*

Cite This: *ACS Appl. Polym. Mater.* 2024, 6, 192−206 Read Online

ACCESS | Metrics & More | Article Recommendations | Supporting Information

**ABSTRACT:** Antioxidant and intelligent poly(lactic acid)-*n* (PLA-*g*-Cur) was synthesized by peroxide-initiated reactive extrusion as a low-cost, sustainable packaging material to reduce the economic and environmental burden of food and plastic waste. The superior mechanical properties of PLA-*g*-Cur compared to radically processed PLA without curcumin suggested antioxidant stabilization of PLA-*g*-Cur that inhibited the degradation of the polymer backbone. These results were supported by an increased onset decomposition temperature ($T_{95}$) from 315 °C for PLA to 334 °C for PLA-*g*-Cur, highlighting enhanced thermal stability. Migration values for PLA-*g*-Cur films were >160× below the EU migratory limit for food contact polymers (0.1 mg/cm$^2$), supporting the use of PLA-*g*-Cur packaging in a wide range of food applications. Modified PLA blocked >93% of UV light while maintaining 89% visible light transmittance, demonstrating the potential to inhibit photooxidation while maintaining material transparency. Significant radical scavenging and spoilage indicating performance of PLA-*g*-Cur further supported this method as an industrially scalable technology to reduce food and plastic waste.

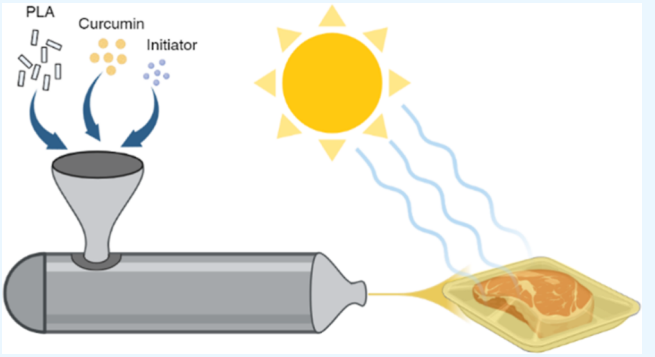


**KEYWORDS:** *active packaging, intelligent packaging, reactive extrusion, nonmigratory, biodegradable, curcumin, antioxidant*



## INTRODUCTION

The United Nations FAO estimated that food waste accounted for nearly one-third of the global food supply, corresponding to approximately 28% of agricultural land use.[1] Low-cost, sustainable solutions are thus needed to mitigate the greenhouse gas emissions, agricultural landfills, and economic loss caused by food waste. Active and intelligent packaging are emerging technologies that can be used to extend the shelf life of products through the inhibition and indication of food spoilage. Active packaging incorporates functional compounds such as antioxidants, antimicrobials, and moisture scavengers directly into the packaging material. Because functional compounds are not dispersed throughout the bulk product like direct additives, active packaging can extend the lifetime of functionality and decrease the amount of additives necessary for effective preservation.[2] Intelligent packaging can inform consumers and retailers of spoilage by visual or quantitative color change in response to external stimuli such as microbial growth, which can mitigate food loss by tracking product freshness throughout the supply chain. Integration of active and intelligent compounds into biodegradable plastics would be an effective strategy to mitigate the converging environmental and economic impacts of both food and plastic waste. Indeed, food and packaging/containers comprise nearly 45% of the materials landfilled in the United States, highlighting the environmental burden of food and packaging waste.[3] Furthermore, the majority of petroleum-based plastics [such as polypropylene (PP), polystyrene, and polyethylene] are not recycled and thus accumulate in landfills or the environment, where they break down into microplastics that contaminate the environment through bioaccumulation. It is predicted that by 2050, the weight of plastic in the ocean will exceed that of fish,[4] underscoring the urgent need for more sustainable materials to displace the reliance on single-use petroleum-based plastics. The production of poly(lactic acid) (PLA), a bioderived and biodegradable thermoplastic polyester, has been reported to lead to 15−60% less carbon emissions and 25−50% less energy consumption (on an overall life cycle analysis basis) than petroleum-based polymers. In addition to thermoformability, biocompatibility, and mechanical strength, these environmental benefits have rendered PLA one of the most widely adopted biodegradable polymers in the packaging industry.[5] Therefore, the development of active and intelligent PLA packaging could be an effective strategy to add value to biodegradable polymers and reduce both food and plastic

Received: August 9, 2023
Revised: November 14, 2023
Accepted: November 16, 2023
Published: December 5, 2023

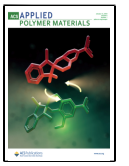

waste. However, thermal degradation during extrusion and inferior water barrier properties of PLA limit the replacement of its petroleum-based counterpart, polyethylene terephthalate (PET), in widespread packaging applications.[6] Modification of PLA with active ligands that add a preservative and/or indicate functionality and reduce thermal degradation could expand the use of PLA over PET packaging.

Extrusion is an efficient, continuous, and uniform manufacturing process used in a wide range of industries. Reactive extrusion enables covalent modification of polymers through a solvent-free process by thermally catalyzed reactions such as radical grafting by peroxide initiation.[7] Radical functionalization has been used extensively to tune the properties of commodity plastics, such as grafting of PP with maleic anhydride (MA) to improve interfacial adhesion,[8] reactive compatibilization of starch composite materials,[9] and modification of polyethylene with vinyl monomers to increase reactivity.[10] Recently, reactive extrusion has been explored as a scalable method to fabricate active and intelligent packaging by the covalent modification of materials with functional ligands. By immobilizing the functional ligands by covalent linkages, these packaging materials may be considered nonmigratory, with potential advantages over migratory alternatives. For instance, whereas nonreactive blending of active compounds into polymer matrices can result in undesired changes in the organoleptic properties of the packaged good (e.g., strong odorants in the case of compounded essential oils), binding the active compounds to the polymer matrix limits the likelihood of migration to the packaged product. Additionally, since immobilized active compounds are unlikely to enter the product matrix, they could be regulated as food contact materials rather than food additives, a potential regulatory benefit.[2] Reactive extrusion thus offers a scalable method to produce nonmigratory active and intelligent packaging; however, the functionalization of biodegradable polyesters like PLA remains a challenge in the plastics industry.[11]

Reactive extrusion offers a scalable and solvent-free method to improve the water barrier properties and the preservative functionality of PLA through covalent modification. However, thermal processing can lead to the degradation of PLA by chain scission and cross-linking, mechanisms that are exacerbated by the presence of radical initiators.[12] The addition of phenolic compounds during PLA processing can inhibit these degradative mechanisms through radical stabilization of reactive oxygen species (ROS) that are responsible for thermal oxidation of the polymer backbone.[13] For instance, Irganox 1010, a common synthetic polyphenol used in polymer processing, has been shown to retard the degradation of PLA during hot melt extrusion.[14] Additionally, natural phenolic compounds such as protocatechuic acid,[15] rosemary essential oil,[16] and thymol[17] have been reported to enhance the thermal stability and mechanical and water barrier properties of PLA through plasticization, cross-linking, and compatibilization. Therefore, incorporation of phenolic compounds in the reactive extrusion of PLA could enhance the thermal, mechanical, and water barrier properties while limiting thermal degradation of the polymer backbone. However, the extrusion process must be carefully designed such that the radical quenching offered by the phenolics during extrusion to protect against polymer degradation does not inactivate the antioxidant function of the phenolic for use in active packaging applications.

Curcumin is a natural polyphenol extracted from *Curcuma longa* L. (turmeric) with traditional use as a therapeutic agent in pharmaceuticals. Due to its reported antioxidant, antimicrobial, anti-inflammatory, and color-changing properties, curcumin has garnered interest as a bioactive compound for active and intelligent packaging.[18] The antioxidant capacity of curcumin can be attributed to the radical scavenging activity of curcumin's phenol and keto-enol groups and resonance stabilization of radical structures.[19,20] The most common synthetic antioxidant food additives such as butylated hydroxyanisole (BHA), butylated hydroxytoluene (BHT), propyl gallate, and *tert*-butyl hydroquinone are suspected of causing adverse health effects, highlighting the potential advantage of curcumin as a natural and safe alternative to synthetic antioxidants.[21] The antioxidant performance of curcumin-based active materials has been validated in a variety of polymers and food systems. For instance, de Campos et al. demonstrated the inhibition of oil oxidation by TPCS/PBAT films containing curcumin,[22] and Shen et al. reported a reduction in pork lipid oxidation by chitosan/curcumin nanoparticles.[23] Additionally, curcumin can change color under alkaline conditions by deprotonation of the phenol and keto-enol groups, resulting in a shift of the visible light absorbance maximum from 428 nm (yellow curcumin) to 467 nm (red curcumin).[18] Bacterial growth on meat and seafood leads to the release of total volatile basic nitrogen (TVBN) compounds, which can interact with curcumin-based intelligent packaging to indicate spoilage to consumers and manufacturers. Cvek et al. demonstrated color change of PLA/poly(propylene carbonate) (PPC) curcumin films in response to shrimp spoilage,[24] Yildiz et al. monitored chicken freshness with curcumin-based chitosan/poly(ethylene oxide) packaging,[25] and Liu et al. displayed color indication of pork spoilage with κ-carrageenan/curcumin films.[26] Additionally, curcumin has been reported to enhance the mechanical and water vapor barrier properties of biopolymers by imparting increased compatibility and hydrophobicity.[26] While curcumin has been used extensively in migratory packaging to confer active and intelligent functionality, to the best of the authors' knowledge, curcumin has never been covalently grafted to a biodegradable polymer toward the long-range goal of active and intelligent biomaterial packaging to reduce the converging environmental burden of food and petroleum plastic waste.

The aim of this work was to develop antioxidant and intelligent biodegradable packaging through the immobilization of curcumin on PLA via reactive extrusion. Previous work has demonstrated successful radical modification of PLA by tertiary hydrogen abstraction[27] and of phenolic compounds by phenol hydrogen abstraction.[28,29] Thus, we predicted that peroxide-initiated radical extrusion would enable the covalent modification of PLA with curcumin. We hypothesized that functionalization of PLA would engender antioxidant and color-changing activity while limiting the thermal degradation of material properties. This work demonstrates a scalable method to manufacture functional biodegradable materials with conserved physical properties, introducing a commercially translatable technology to reduce the negative impacts of food and plastic waste.

## MATERIALS AND METHODS

**Materials.** 2,2′-Azino-bis(3-ethylbenzothiazoline-6-sulfonic acid) diammonium salt (ABTS, 98%), buffered peptone water (10 g peptone/L), and sodium hydroxide (≥97%) were bought from Fisher



https://doi.org/10.1021/acsapm.3c01820
ACS Appl. Polym. Mater. 2024, 6, 192−206

**Scheme 1. Proposed Radical Grafting Reaction between PLA and Curcumin by Peroxide Initiation under Extrusion Conditions**[a]

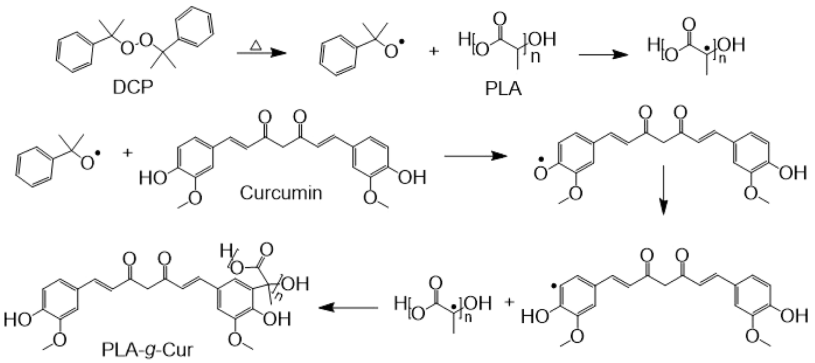


[a]Alternative mechanisms and byproducts are not displayed but may include grafting of curcumin by phenoxy or enol alkoxy radical to the tertiary carbon of PLA.

Scientific (Fair Lawn, NJ). 100% waterproof quick-drying silicone sealant (Henkel, IDH: 2764352) was purchased from Home Depot (Ithaca, NY). Dicumyl peroxide (DCP, 98%) was sourced from Krackeler Scientific and homogenized into a fine powder with a mortar and pestle. Ethanol (EtOH, 200 proof) was purchased from Decon Laboratories (King of Prussia, PA). Aluminum crimp caps (20 mm diameter), ammonia solution (28−30%), curcumin (synthesis grade, cat no. 8.20354, CAS no. 458-37-7), 2,2-diphenyl-1-picrylhydrazyl (DPPH, ≤100%), glacial acetic acid (99.7%), and 10 mL headspace glass vials (23 mm O.D. × 46 mm H× 12.5 mm I.D.), hydrochloric acid (trace-metal grade), (±)-6-hydroxy-2,5,7,8-tetramethylchromane-2-carboxylic acid (Trolox, 97%), polytetrafluoroethylene (PTFE)/butyl septa (20 mm diameter × 3.42 mm thickness), potassium persulfate (≥99%), sodium acetate trihydrate (≥99%), sodium phosphate dibasic heptahydrate (≥98%), and sodium phosphate monobasic monohydrate (≥98%) were acquired from Millipore Sigma (Burlington, MA). Verdana USDA Certified Organic Coconut MCT Oil—fractionated coconut oil (100%) and 1 oz clear PET jars with Styrofoam septa (1.96″ L × 1.96″ W × 1.33″ H) were purchased from Amazon.com (Seattle, WA). Unpeeled shrimp (14.6 ± 2.6 g) from the North Carolina coast were procured from a local grocery store (Ithaca, NY). Plate count agar (PCA) was purchased from HiMedia Laboratories (Kennett Square, PA). PLA pellets (Ingeo Biopolymer 7001D) were acquired from NatureWorks (Minnetonka, MN, USA). Grades U, E, and EX purges for the extruder were generously supplied by Asahi Kasei Asaclean Americas (Parsippany, NJ, USA). All reagents were used as received without further processing.

**Synthesis of Poly(lactic acid)-*graft*-Curcumin.** *Preparation of Poly(lactic acid) Granules and Control Films.* Prior to radical grafting, PLA pellets were first extruded and pelletized into 0.5 mm granules, as described previously, to facilitate better mixing with reagent powders.[30] First, PLA pellets were dried in a gravimetric oven at 80 °C for 4 h to remove excess moisture according to the manufacturer's guidelines and used immediately or stored over calcium sulfate desiccant until future use. Next, an attached volumetric feeder (11 mm volumetric single screw feeder for process 11 [MK2] by Thermo Electron, Germany) was used to feed dried PLA pellets at 10% the maximum rate into a Process 11 Parallel Twin Screw Extruder (Thermo Fisher Scientific, Waltham, MA, USA). PLA strands were extruded at 150 rpm through a 1.5 mm die using the following temperature profile: zone 2—145 °C, zone 3—190 °C, zone 4—200 °C, zone 5—200 °C, zone 6—200 °C, zone 7—200 °C, zone 8—200 °C, and 210 °C at the die. A VariCut pelletizer (Thermo Fisher Scientific, Waltham, ME) was set at L1 to form 0.5 mm granules out of the PLA filaments. PLA granules were stored over calcium sulfate desiccant for at least 24 h prior to hot pressing. To form polymer films, 2 g of granulated PLA (gPLA) was placed in a single layer between two 5 mil Kapton films (Cole-Parmer, Vernon Hills, IL) and allowed to melt in a heated four-post manual hydraulic press (Carver, Wabash, IN) at 180 °C for 2 min. Films were pressed for 5 min at a force of 1500 lbf to achieve a final thickness of 0.14−0.19 ± 0.02 mm across the film. Thickness was measured using a SnapThick (iGAGING, San Clemente, CA) 3-Way Digital Electronic Thickness Gauge accuracy of 0.02 mm. Films were then fully immersed in 100% EtOH and washed at 150 rpm for 2 h to remove surface contaminants. The films were dried with a filtered compressed air gun and stored over anhydrous calcium sulfate desiccant until further use. The filter in the air gun was an in-line high-volume low-pressure (HVLP) filter to remove oil, aerosols, smoke, solids, and condensed moisture (TCP Global, MF-201).

*Preparation of Functionalized PLA (PLA-g-Cur) Via Reactive Extrusion.* gPLA, DCP, and curcumin were used to create active and intelligent PLA-*g*-Cur via radical grafting (Scheme 1, made with ChemDraw 20.1 by PerkinElmer, USA) by reactive extrusion based on similar methods to those described previously.[31] A mortar and pestle was used to grind DCP flakes into a fine, homogeneous powder, which was stored at 4 °C until further use. gPLA was mechanically mixed with 0.5% w/w powdered DCP and 0.5, 1, or 2% w/w curcumin and fed into the extruder at 18%, the maximum rate. Mixtures containing 0.5, 1, and 2% w/w curcumin and gPLA without DCP were also extruded as ungrafted controls for the immobilization of curcumin. A mixture containing gPLA and 0.5% w/w DCP was also extruded as a control for changes in mechanical properties caused by radical cross-linking or chain scission. Each sample was extruded at 150 rpm through a 1.5 mm die under the following conditions: zone 2—145 °C, zone 3—160 °C, zone 4—165 °C, zone 5—170 °C, zone 6—180 °C, zone 7—185 °C, zone 8—195 °C, and 210 °C at the die. Zones 3, 4, and 6, contained screw mixing elements, while the rest of the zones contained screw conveying elements. Sample filaments were granularized using the same pelletizer parameters as described for gPLA. The pressing procedure was the same as described for gPLA; however, the pressing force was modified for each polymer to achieve 0.14−0.19 mm thickness across films due to variations in melt viscosity. The pressing pressure used for each sample is listed in Table 1. Polymer films were washed, dried, and stored under the same conditions as those described for gPLA. The nomenclature is as follows: PLA-*g*-Cur*X* for samples extruded with DCP and PLA/Cur*X* for samples extruded without DCP, where *X* refers to the curcumin concentration (% w/w), and slashes signify unreacted blends (melt blended without radical grafting). Cross-linked PLA is referred to as cPLA, for samples processed with DCP but without curcumin (Table 1).

**Chemical, Interfacial, and Mechanical Characterization of PLA-*g*-Cur Films.** *Attenuated Total Reflectance Fourier Transform Infrared Spectroscopy.* An IRPrestige FTIR spectrometer fit with a diamond ATR crystal (Shimadzu Scientific Instruments Inc., Kyoto, Japan) was used to observe the characteristic functional groups of curcumin in treated and control films. The diamond crystal was cleaned by a swab dampened with 100% EtOH prior to use. The


https://doi.org/10.1021/acsapm.3c01820
ACS Appl. Polym. Mater. 2024, 6, 192−206

**Table 1. Concentration (% w/w) of DCP and Curcumin in gPLA for Each Sample and Pressing Force (lbf) Used to Melt Polymer Granules into Films[a]**

| sample ID | DCP % (w/w) | curcumin % (w/w) | pressing force (lbf) |
|---|---|---|---|
| gPLA | 0 | 0 | 1500 |
| cPLA | 0.5 | 0 | 4000 |
| PLA-*g*-Cur0.5 | 0.5 | 0.5 | 2500 |
| PLA-*g*-Cur1 | 0.5 | 1 | 1500 |
| PLA-*g*-Cur2 | 0.5 | 2 | 1500 |
| PLA/Cur0.5 | 0 | 0.5 | 1500 |
| PLA/Cur1 | 0 | 1 | 1500 |
| PLA/Cur2 | 0 | 2 | 1500 |

[a]The remaining weight percent is comprosed of gPLA.

average of 32 scans taken at 4 $cm^{-1}$ resolution and using Happ-Genzel apodization was used for each sample with air as the background spectrum. PLA-*g*-Cur spectra were compared against cPLA and gPLA negative control spectra, and baseline corrections and plotting were performed on an Origin Pro 2021b (OriginLab Corp., Northampton, MA).

*Advancing and Receding Water Contact Angles.* An Attention theta optical tensiometer (Biolin Scientific, Stockholm, Sweden) was used to analyze the wettability of treated and control films by the dynamic water contact angle based on methods previously reported.[31] In brief, ~4 $\mu$L of distilled water was deposited on the surface of each sample, with contact angle values recorded during droplet deposition and withdrawal. For the advancing contact angle, the syringe was inserted into the droplet and water was injected at a rate of 0.5 $\mu$L/s with images recorded at 14 frames per second. The Young−Laplace method was used to analyze the advancing contact angle, which was defined as the maximum mean contact angle before the droplet's baseline increased. For the receding contact angle, the syringe was reinserted into the expanded droplet, and the volume of the droplet was decreased at a rate of 0.5 $\mu$L/s with images recorded at 14 frames per second. The receding contact angle was defined as the minimum mean contact angle before the droplet's baseline decreased. For each sample, the receding contact angle was subtracted from the advancing contact angle to determine hysteresis. The water contact angle was evaluated on two different spots on each of two different films for two independently extruded batches of each sample (with extrusion performed on different days), totaling eight replicates per sample.

*Mechanical Testing of Films.* Mechanical testing was conducted using an Instron 5566 Universal Testing Machine (Instron, Norwood, MA, USA) using methods adapted from ASTM D882-18.[32] Samples were cut into a dumbbell shape with a gauge length of 26 mm. The separation rate of the grippers was set to 12.5 mm/min with a maximum separation of 40 mm, and a stress−strain curve was plotted automatically by Bluehill Universal Software (Instron, Norwood, MA, USA). Young's modulus was determined by the initial slope of the stress−strain curve, the tensile strength was determined as the peak of the curve, and the elongation at break was determined by dividing the maximum length before break by the initial length of the film (26 mm) and multiplying by 100. Mechanical testing was performed in triplicate from a single extruded batch of each sample.

*Water Vapor Permeability.* Water vapor permeability (WVP) was analyzed using an assay adapted from the ASTM E96/E96M-16 Water Method.[33] In brief, films were cut into 2 × 2 $cm^2$ coupons, and the average thickness of four random points on each coupon was recorded. Films were sealed using 100% waterproof quick-drying silicone sealant (Henkel, IDH: 2764352) to the 12.5 mm diameter mouth of 10 mL glass headspace vials filled with 7.6 mL of DI water (Figure S3). The 7.6 mL volume equated to 19 mm of space between the film and the surface of the water and created essentially a 100% relative humidity (RH) environment within the vials. Sample vials were placed in a desiccator filled with a combination of calcium sulfate desiccant and silica gel and allowed to equilibrate for 2 h at 32.2 °C. After equilibration, vials were weighed on an analytical balance with up to 0.0001 g precision, and these values were recorded as the starting mass. Vials were placed back in the desiccator with a humidity reader to ensure between 0 and 5% RH (±5% RH accuracy) during incubation. The desiccator was placed in an incubator at 32.2 °C for 6 days, and vials were measured for mass loss every 24 h. Water vapor transmission rate (WVTR, g/$m^2$ s) was determined by dividing the slope of mass (g) loss over time (s) by the area of the exposed film (0.0001227 $m^2$). WVP (eq 1) was determined by

$$\mathrm{WVP} = \mathrm{WVTR} \times L/S\ (R_1 - R_2) \quad (1)$$

where WVTR is in g/$m^2$ s, $L$ is the thickness across the film (m), $S$ is the saturation vapor pressure at test temperature (Pa), and $R_1$ and $R_2$ are the RH values (expressed as decimals) of the inside of the vials and inside the desiccant chamber, respectively.[34] The saturation vapor pressure of water at 32.2 °C is 4814 Pa. The average RH of the desiccator at all six time points was 2%, so an $R_2$ value of 0.02 was used for calculations. $R_1$ was estimated as 1.00 based on the assumption of 100% RH within the vials. WVTR and WVP were determined for each individual coupon, and analysis was performed on quadruplicate coupons for each sample. Isotactic PP was included as a control material known to have a low WVP to validate adaptation of the method.

*Thermal Analysis.* Thermogravimetric analysis (TGA 5500, TA Instruments, New Castle, DE, USA) was used to evaluate the thermal stability of samples. Films and curcumin powder were heated in platinum pans at 10 °C/min to 600 °C under nitrogen. For differential scanning calorimetry (DSC 2500, TA Instruments, New Castle, DE, USA), a heat−cool−heat recipe was performed on films and curcumin powder sealed in aluminum pans with a heating and cooling rate of 10 °C/min from −20 to 190 °C. All thermal analyses were performed on a single representative sample for each treatment and analyzed using TRIOS 5.1.1 software (TA Instruments, New Castle, DE, USA).

*Migration Assay in Food Simulants.* A standard migration assay based on EU and FDA recommendations for food contact materials was used to validate curcumin immobilization in functionalized films.[35,36] Films were cut into 1 × 2 $cm^2$ coupons and placed in 10 mL glass headspace vials with polytetrafluoroethylene−butyl (PTFE−butyl) septum and crimp-top aluminum seals. Each vial was filled with 10 mL of the following food simulants: DI water was used to represent aqueous foods, 10% EtOH was used to represent low alcohol foods, 3% acetic acid was used to represent acidic foods, and fractionated coconut medium chain triglyceride (MCT) oil was used to represent fatty foods. After vials were incubated for 10 days at 40 °C, aliquots were evaluated by a Synergy Neo2 Hybrid Multi-Mode Reader (BioTek Instruments, Winooski, VT) at 428 nm, which was verified as the peak absorption wavelength for curcumin solutions (Figure S7). A curcumin stock solution (0.1 mg/mL in 100% EtOH) was diluted in each simulant to produce curcumin standard curves for the colorimetric quantification of curcumin migration, with each simulant used as a blank for each standard curve (Figure S8). Each standard curve was made in triplicate with a limit of detection of 0.000125 mg/mL, and calculated curcumin migration from each film was compared to the established migratory limit for food contact materials by the European Union (10 mg/100 $cm^2$).[35] For each simulant, migratory analysis was performed on triplicate coupons from each of two independently extruded batches of each sample, totaling six replicates per treatment.

*Curcumin Migration from Ungrafted Control Films during Ethanol Incubation.* To determine the importance of DCP in the immobilization of curcumin onto PLA, films were incubated in EtOH to compare the leaching of unbound curcumin between the control and sample polymer. Films were cut in 1 × 1 $cm^2$ coupons, and two coupons were placed in a well of a 24-well plate. The coupons were covered with 1 mL of 100% EtOH, and the plates were sealed with parafilm and the plate lid. Aluminum foil was wrapped around the plate to prevent light degradation of curcumin color, and plates were incubated at 25 °C with aliquots taken at 30 min and 1, 2, 4, and 24 h. Aliquots were analyzed on a Synergy Neo2 Hybrid Multi-Mode Reader (BioTek Instruments, Winooski, VT) at 428 nm, and the


https://doi.org/10.1021/acsapm.3c01820
ACS Appl. Polym. Mater. 2024, 6, 192−206

curcumin concentration was quantified with a standard curve made in 100% EtOH. The leaching assay was performed in triplicate for each of two independently extruded batches of material, totaling six replicates per treatment. Values were plotted and fit to a sigmoidal dose−response curve on GraphPad Prism 9.3.0 (La Jolla, CA).

*UV−visible Light Properties.* The UV-blocking and visible transparency properties of functionalized materials were determined by UV−vis spectrophotometry using a Synergy Neo2 Hybrid Multi-Mode Reader (BioTek Instruments, Winooski, VT). Samples were cut into 14 in. circles using a standard hole punch and placed in a polystyrene 96-well plate. Each well was analyzed from 280 to 700 nm with 2 nm resolution, the average absorbance of triplicate blank wells containing no sample was subtracted, and absorbance was converted to % transmission and plotted for each wavelength. For data points with absorption above the limit of detection for the spectrophotometer, the highest absorption value among all samples ($A_{max} = 3.5$) was used for calculations. UV−vis analysis was performed on three coupons for each of the two independently extruded batches of each sample, totaling six replicates per treatment.

**Antioxidant and Color-Changing Performance of PLA-*g*-Cur Films.** *ABTS and DPPH Radical Scavenging Assays.* Colorimetric 2,2′-azino-bis(3-ethylbenzothiazoline-6-sulfonic acid) ($ABTS^{\bullet}+$) and 2,2-diphenyl-1-picrylhydrazyl radical ($DPPH^{\bullet}$) assays were used to quantify the antioxidant properties of PLA-*g*-Cur films, based on methods from previous work.[31] In brief, a 7 mM solution of ABTS and a 2.45 mM solution of potassium persulfate were each made in 4 mM phosphate buffered saline (PBS, pH 7.4). These solutions were mixed in a 1:1 ratio, and the mixed solution was allowed to develop for 16 h. The developed solution was diluted with 4 mM PBS (pH 7.4) to an absorbance of 0.70 ± 0.30 at 734 nm to produce the ABTS working solution. Control and treated films were cut into 1 × 1 $cm^2$ coupons and incubated in a 24-well plate with 0.5 mL working ABTS solution mixed with 0.5 mL 4 mM PBS (pH 7.4). The plate was incubated at 30 °C for 24 h with shaking at 150 rpm. An aliquot of each sample was analyzed on a Synergy Neo2 Hybrid Multi-Mode Reader (BioTek Instruments, Winooski, VT) at 734 nm. For the DPPH assay, 1 × 1 $cm^2$ coupons were incubated in a 24-well plate with 0.5 mL DPPH solution (0.1 mM in 100% EtOH) and 0.5 mL DI water to achieve a 50% EtOH incubation matrix. The plate was incubated at 25 °C for 24 h with shaking at 150 rpm. An aliquot of each sample was analyzed at 517 nm. Radical scavenging capacity was determined by a Trolox standard curve from 0 to 30 μM in 4 mM PBS (pH 7.4) and 50% EtOH to achieve Trolox equivalent antioxidant capacity (TEAC) for ABTS and DPPH, respectively. The average TEAC of the blank controls (samples containing no films) was subtracted from the TEAC of each of the samples to account for any color loss of the radical solution during the assay. ABTS and DPPH were performed on quadruplicate coupons from each of two independently extruded batches of the material, totaling eight replicates per sample.

*Color Changing Response to Ammonia.* To analyze the intelligent properties of PLA-*g*-Cur films, coupons were exposed to an ammonia solution and analyzed for visible and quantitative color change based on previously reported methods.[31] In brief, 1.2 × 1.2 $cm^2$ coupons were attached by double-sided Kapton tape to the PTFE−butyl septa of aluminum caps for 10 mL headspace vials. The vials were filled with 9 mL of 0.8 M ammonia solution, crimped to prevent leakage, and incubated at room temperature (~22 °C) for 24 h to allow the development of ammonia vapors. Coupons were analyzed before and after incubation by a CR-400 Chroma Meter (Konica Minolta Sensing, Ramsey, NJ) using CIELab color space parameters to detect color change, and digital images were taken in a lightbox. Total color change ($\Delta E^*$, eq 2) and the change in chromatic parameter ($\Delta C^*$, eq 3) of each coupon was calculated

$$\Delta E^* = \sqrt{(L_1^* - L_2^*)^2 + (a_1^* - a_2^*)^2 + (b_1^* - b_2^*)^2} \quad (2)$$

$$\Delta C^* = \sqrt{(a_1^* - a_2^*)^2 + (b_1^* - b_2^*)^2} \quad (3)$$

where $L^*$ indicates lightness, $a^*$ indicates redness/greenness, and $b^*$ indicates blueness/yellowness. Color change analysis was performed on triplicate coupons from two independently extruded batches, totaling six replicates per treatment. A random number generator was used to pick a digital image representative of each treatment reported here, and the images were cropped square to maximize the area shown.

*Color Changing Response to Shrimp Spoilage.* To demonstrate the intelligent properties of treated films in real applications, the bacterial count of shrimp was compared to the color change of PLA-*g*-Cur films during storage. The shrimp used in this study were purchased from a local grocery store the day of receiving the shipment, which was guaranteed to be less than 24 h since procurement from the ocean. Shrimp were maintained at 4 °C, and experiments were performed the same day as purchase. The tail, legs, and shell were removed, and the shrimp were deveined prior to washing in DI water. Shrimp of a similar size (by weight) and appearance were packaged in 1-oz PET jars with screw lids fit with Styrofoam septa to prevent leakage. PLA-*g*-Cur2 films were cut into 2 × 2 $cm^2$ coupons, and initial CIELab color measurements were recorded with a CR-400 Chroma Meter (Konica Minolta Sensing, Ramsey, NJ). Coupons were taped to the inside of the jar lids to facilitate headspace interaction without shrimp contact, and all jars were incubated at 4 °C. Triplicate jars were pulled every 12 h, and color measurements of the coupons were recorded. Each shrimp was diluted with a 4:1 ratio of sterilized water (mL)/shrimp (g) and stomached in a Whirl-Pak filter bag at 260 rpm for 1 min. An aliquot of the filtrate was serially diluted in 0.1% peptone water, and 100 μL of the appropriate dilution was plated in duplicate on PCA. Plates were incubated at 30 °C for 48 h, and plates containing between 30 and 300 cfu were counted. The average count of duplicate plates was recorded as the total viable count (TVC) for each shrimp. Initial TVC of shrimp prior to incubation was recorded as well, and all analyses were performed on triplicate shrimp. Change in $\Delta C^*$ of films was calculated (eq 3) and compared to TVC. Values were plotted and fit to a sigmoidal dose−response curve on GraphPad Prism 9.3.0 (La Jolla, CA).

**Statistical Analysis.** PLA-*g*-Cur was synthesized in duplicate batches on independent days, and all values represent means of individual determinations, in which half of the determinations were on each of two independently synthesized batches of material. The normal distribution of each result was confirmed by the Shapiro−Wilk test, and statistical significance between samples was determined using analysis of variance (ANOVA) with Tukey's HSD multiple comparisons ($p < 0.05$) on GraphPad Prism 9.3.0 (La Jolla, CA).

## RESULTS AND DISCUSSION

**Synthesis of Poly(lactic acid)-*graft*-Curcumin.** Peroxide-initiated radical grafting is a common strategy to functionalize polymers with active ligands and tailor polymer properties to target applications.[7] The reaction begins with the thermal decomposition of the peroxide initiator into identical alkoxy radicals, which can abstract a hydrogen from the polymer backbone to form a polymer macroradical. In polymers presenting a tertiary carbon (including PLA), hydrogen abstraction preferentially occurs from the tertiary carbon, as proposed in Scheme 1. Similarly, curcumin can undergo hydrogen abstraction from either of its phenol groups followed by an intermolecular hydrogen transfer that moves the radical to the ortho or para position of the aromatic ring relative to the hydroxyl.[28,29] Alternatively, curcumin is susceptible to abstraction of the carbon-centered hydrogen of the β-diketone moiety, which can also undergo an intermolecular hydrogen transfer to form an enolic alkoxy radical.[37] Thus, curcumin can react with DCP to form a phenoxy radical, benzyl radical, or enolic alkoxy radical that can react with the polymer macroradical to generate the


https://doi.org/10.1021/acsapm.3c01820
ACS Appl. Polym. Mater. 2024, 6, 192−206

grafted product. While only one product is proposed here (Scheme 1), alternative reaction pathways are noted in our previous work,[31] demonstrating PLA grafted to the phenol, keto-enol, and aromatic ring of curcumin.

While the radical scavenging capacity of curcumin motivates its use in active packaging, it also poses a challenge to standard radical grafting conditions, demanding an innovative synthesis approach to obtain the grafted product. Due to its radical-stabilizing resonance, curcumin can preferentially scavenge DCP radicals compared to the PLA tertiary carbons. In reactive extrusion, the reactivity is limited to reagents in the melt. Consequently, if all of the reagents entered the reactive extrusion melt at the same time, curcumin would immediately quench the peroxide radicals, inhibiting the formation of the PLA macroradicals and thus the grafted product. Therefore, we leveraged our knowledge of reagent melting temperatures and extrusion parameters to design a temperature profile that would maximize synthesis of the desired product. The initial mixing zones (zones 3 and 4) were maintained below the melting temperature of curcumin (179 °C) and above the melting temperature of PLA (148 °C). In these initial zones, the DCP radicals preferentially abstract hydrogens from the melted PLA. The melted PLA could exclusively react with the DCP radicals to form polymer macroradicals, while curcumin was mixed within the polymer matrix as a solid powder. Unmelted curcumin could only have limited interactions with DCP radicals due to the aggregation of solid particles, reducing the potential for radical quenching and maximizing the formation of PLA macroradicals. In the final mixing zone (zone 6), the temperature was increased above the melting point of curcumin, allowing for curcumin radical formation with the remaining DCP and covalent immobilization on the PLA macroradicals. The temperature profile was kept close to the melting temperatures of the reagents to minimize thermal degradation.[38]

The curcumin concentration used for PLA-*g*-Cur material was based on previous research in migratory active packaging, which demonstrated potent UV-blocking, antioxidant, and color-changing performance with curcumin concentrations between 0.25 and 2% w/w.[24,39] Initial experiments were conducted to analyze the effect of drying PLA prior to extrusion. We hypothesized that while drying PLA prior to extrusion would prevent hydrolysis and degradation of mechanical properties, increasing the number of hydroxyl end groups could improve immobilization by radical grafting and hydrogen bonding interactions. However, preliminary migration studies showed no significant differences between drying and not drying PLA prior to extrusion. Consequently, all extrusions for this work were performed with dried PLA to minimize potential degradation of mechanical properties by hydrolysis.

**Chemical, Interfacial, and Mechanical Characterization of PLA-*g*-Cur Films.** *Attenuated Total Reflectance Fourier Transform Infrared Spectroscopy.* Attenuated total reflectance Fourier transform infrared (ATR−FTIR) spectroscopy was used to confirm the presence of curcumin in PLA-*g*-Cur films (Figure S1). Full spectra display the characteristic absorption bands of PLA, such as the symmetric and asymmetric stretching of the C−O−C group (1180 and 1080 $cm^{-1}$, respectively), asymmetric and symmetric C−H vibrations of the methyl group (1452 and 1359 $cm^{-1}$, respectively), and C═O stretching vibrations of the ester group (1747 $cm^{-1}$).[39] A magnified spectrum of the curcumin fingerprint region exhibits new absorption bands at 1514 $cm^{-1}$ characteristic of mixed vibrations between C═C and C═O groups in the 1,3-diketone-conjugated carbonyl unique to the curcumin. Other functional groups are difficult to distinguish, likely due to the low percentage of curcumin compared to that of PLA and the structural similarities of key functional groups that present the most dominant absorbances in curcumin and PLA (e.g., carbonyl, hydroxyl, and ether). An interesting observation is the absorption band shift from 1633 $cm^{-1}$ for gPLA and cPLA to 1625 $cm^{-1}$ for all PLA-*g*-Cur films. As this band is characteristic of C═O stretching in PLA,[40,41] it is possible that the downward shift is due to the hydrogen bonding between PLA carbonyls and the curcumin phenols.[42] The subtle increase in absorbance in this region may also be attributed to the C−H bending frequency of the aromatic group unique to the curcumin. The increased absorbances observed in the spectra of PLA-*g*-Cur compared to those in the spectra of cPLA and gPLA support the presence of key functional groups (conjugated carbonyl and aromatic group) in curcumin but not in PLA and are in agreement with other reports.[43]

*Advancing and Receding Water Contact Angles.* Dynamic water contact angles were used to analyze the wettability of PLA-*g*-Cur materials (Table 2). Compared to the static contact angle, dynamic measurements take into account the chemical/physical heterogeneity of a material and provide more information on the dry−wetting properties and interfacial adhesion forces of a surface. The advancing contact angle ($\theta_A$) is representative of a material's hydrophobicity and was quantified as the maximum contact angle before the baseline of the water droplet expanded on the polymer surface. Results align closely with advancing water contact angles previously reported for PLA,[30] which demonstrate slightly hydrophilic character (as hydrophobic materials are defined as having $\theta_A > 90°$). Some wettability is expected due to hydrogen bonding between PLA functional groups and water. There was no significant difference between treated and control films, which suggests that the interfacial properties of PLA were conserved with the immobilization of curcumin. Since the advancing contact angle can represent a material's susceptibility to wetting, the sustained hydrophilic character of treated PLA packaging may allow strong interaction with aqueous products, suggesting potential preservative function in applications such as juice, dairy, and condiment packaging.

Receding contact angle ($\theta_R$) provides a measure of the adhesion force at the polymer/water interface and was

**Table 2. Advancing Water Contact Angle, Receding Water Contact Angle, and Hysteresis Values of PLA-*g*-Cur and Control Films[a]**

| sample ID | advancing contact angle (deg) | receding contact angle (deg) | hysteresis (deg) |
|---|---|---|---|
| gPLA | $83.38 \pm 0.76^{A}$ | $48.16 \pm 3.11^{AB}$ | $35.22 \pm 3.84^{ABC}$ |
| cPLA | $83.47 \pm 1.97^{A}$ | $45.26 \pm 2.44^{A}$ | $38.22 \pm 3.04^{A}$ |
| PLA-*g*-Cur05 | $81.72 \pm 1.92^{A}$ | $47.98 \pm 3.90^{AB}$ | $33.74 \pm 4.08^{BC}$ |
| PLA-*g*-Cur1 | $82.13 \pm 2.07^{A}$ | $46.17 \pm 1.59^{A}$ | $35.96 \pm 1.68^{AB}$ |
| PLA-*g*-Cur2 | $82.12 \pm 2.98^{A}$ | $52.14 \pm 3.24^{B}$ | $29.98 \pm 2.09^{C}$ |

[a]Values represent the mean and standard deviation of eight measurements. Statistically significant differences between sample means for each column are indicated by capitalized letters (Tukey's HSD, $p \leq 0.05$).



https://doi.org/10.1021/acsapm.3c01820
ACS Appl. Polym. Mater. 2024, 6, 192−206

Table 3. Mechanical, Water Vapor Permeability, and Thermal Properties of PLA-*g*-Cur and Control Films[a]

| | Young's modulus (Mpa) | tensile strength (Mpa) | elongation at break (%) | WVP ($\times 10^{-11}$ g/m$^2$ s Pa) | $T_{95}$ (°C) | $T_{50}$ (°C) | $T_m$ (°C) | $T_g$ (°C) | $T_c$ (°C) |
|---|---|---|---|---|---|---|---|---|---|
| curcumin powder | | | | | 226 | 561 | 179 | 67 | |
| gPLA | 4649.3 ± 236.0$^A$ | 51.1 ± 4.2$^A$ | 14.7 ± 2.6$^A$ | 2.06 ± 0.04$^A$ | 315 | 348 | 148 | 58 | 125 |
| cPLA | 4285.3 ± 428.9$^A$ | 55.1 ± 5.8$^A$ | 6.8 ± 0.5$^B$ | 2.30 ± 0.32$^A$ | 250 | 314 | 144 | 57 | 114 |
| PLA-*g*-Cur05 | 4465.3 ± 479.0$^A$ | 55.0 ± 5.0$^A$ | 9.1 ± 0.1$^{AB}$ | 2.10 ± 0.11$^A$ | 275 | 312 | 146 | 59 | 120 |
| PLA-*g*-Cur1 | 4215.4 ± 153.7$^A$ | 52.8 ± 7.6$^A$ | 14.4 ± 2.9$^A$ | 2.12 ± 0.13$^A$ | 334 | 373 | 146 | 58 | 119 |
| PLA-*g*-Cur2 | 4795.8 ± 337.1$^A$ | 49.9 ± 7.8$^A$ | 11.1 ± 2.7$^{AB}$ | 2.24 ± 0.42$^A$ | 330 | 371 | 146 | 58 | 120 |

[a]Mechanical and WVP values indicate the mean and standard deviation of three different coupons for each sample. Thermal analysis was performed on each sample for each treatment. Statistically significant differences between sample means for each column are indicated by capital letters (Tukey's HSD, $p \leq 0.05$).

quantified as the minimum contact angle before the baseline of the water droplet receded on the polymer surface. PLA-*g*-Cur films demonstrated statistically the same receding contact angles as gPLA films, which had a receding contact angle in agreement with prior reports.[30] While it was expected that the hydrophobicity of curcumin would decrease the adhesion force between PLA-*g*-Cur and water, the curcumin concentration in these samples may be too low for an observable effect. Based on the results for PLA-*g*-Cur2 compared to those for other PLA-*g*-Cur films, it is possible that increasing the curcumin concentration would increase the hydrophobicity, but this relationship would need to be further characterized. Additionally, hydrogen bonding between PLA and curcumin may reduce the surface orientation of the grafted ligand, limiting the effect of curcumin on the interfacial properties of the material.

Hysteresis, the difference between advancing and receding contact angles, is reported to represent the chemical heterogeneity and roughness of a surface.[44] For pristine homogeneous surfaces without defect, the hysteresis value would be 0° and directly increase with heterogeneity and roughness. cPLA displayed the highest hysteresis value, likely due to cross-linking and chain scission events that occur during radical grafting of PLA under high-temperature processing.[45] These events could lead to a wide dispersion of PLA oligomers and an increasing number of end groups, which could increase the chemical heterogeneity of the surface. Compared to cPLA, PLA-*g*-Cur films have lower hysteresis values, likely due to a decrease in chemical heterogeneity caused by reduced thermal degradation of PLA. Curcumin could inhibit the cross-linking and chain scission of PLA by preferential scavenging of DCP radicals and PLA macroradicals during reactive extrusion, reducing thermal oxidation of the polymer backbone. Additionally, curcumin can act as a compatibilizer by hydrogen bonding with PLA end groups, thus decreasing the effect of chain scission on the surface roughness. Overall, dynamic water contact angle exhibits the conserved wettability and interfacial properties of PLA-*g*-Cur films compared to gPLA, which could support the commercial translation of modified materials. For instance, compared to the reported dynamic contact angles of other polyesters such as PET ($\theta_A$ = 71.0 ± 1.2, $\theta_R$ = 37.7 ± 1.2),[46] all PLA films demonstrated reduced wettability, which could aid in product release and resistance to biocontamination in packaging applications. Interfacial properties provide insight into the radical processing of PLA, suggesting the potential efficacy of curcumin in preventing thermal degradation of the polymer backbone.

*Mechanical Testing of Films.* Since the primary function of packaging is to provide a physical barrier between products and the environment, the adoption of packaging materials is strongly dependent on mechanical, water barrier, and thermal properties. Mechanical testing was used to evaluate the impact strength, flexibility, and stiffness of PLA-*g*-Cur packaging compared to gPLA and cPLA (Table 3). Young's modulus, the initial slope of the stress−strain curve, and a measure of material stiffness were statistically insignificantly different across samples. Additionally, previous research has reported insignificant change in tensile strength after reactive extrusion of PLA with 0.5% w/w DCP,[47] which aligns with the results observed for cPLA and PLA-*g*-Cur films. While it may be expected that the tensile strength of cPLA would decrease due to chain scission, this effect may be neutralized by the increased strength from cross-linking. The only statistically significant differences in mechanical properties are observed for elongation at break, which is lower for cPLA compared to that for gPLA due to a combination of cross-linking and chain scission that decreases the elasticity of the processed materials.[48] Elongation at break was the same for both gPLA and PLA-*g*-Cur films, suggesting that the thermal degradation observed in cPLA samples is at least partially inhibited by the presence of curcumin. Although the results for mechanical properties were not practically different across samples, the conserved strength and elasticity of PLA-*g*-Cur films in contrast to those of cPLA alludes to the utility of curcumin as a stabilizing agent during reactive extrusion.

*Water Vapor Permeability.* WVP was quantified by the ASTM E96/E96M-16 Water Method, whereby the amount of water transmitted through PLA-*g*-Cur and control films was quantified over time (Table 3).[33] Isotactic PP was also evaluated to compare the water barrier properties of PLA with those of petroleum-based polymers. The WVP value of the PP was 0.11 ± 0.08 ($\times 10^{-11}$ g/m$^2$ s Pa), which highlights the superior barrier properties of PP compared to those of PLA materials.[49] Although we hypothesized that the hydrophobicity of curcumin would enhance the water barrier properties of PLA, there were no significant differences across all PLA films. These findings align with the results of the dynamic water contact angle, which demonstrated no significant difference in the wettability of PLA-*g*-Cur compared to that of gPLA, suggesting that the concentration of curcumin is too low for an observable impact on the barrier properties or wettability. Alternatively, the improvement in barrier properties due to increased hydrophobicity could be neutralized by an increase in free volume of the material with the addition of curcumin, creating a more efficient diffusion path for water vapor molecules.[50] The conserved barrier properties of PLA-*g*-Cur films compared to those of gPLA suggest limited chain scission during radical processing since an increase in end groups would increase the hydrophilicity of the bulk polymer and thus


https://doi.org/10.1021/acsapm.3c01820
ACS Appl. Polym. Mater. 2024, 6, 192−206

WVP.[51] It is promising to note that the radical grafting of curcumin during reactive extrusion can be used to functionalize PLA packaging without a negative impact on mechanical or water barrier properties of the native polymer.

*Thermal Analysis.* TGA and DSC were used to evaluate the thermal stability of treated and control films (Table 3). Curcumin powder begins decomposition at the lowest temperature but displays significant thermal stability of nonvolatile components, maintaining >45% weight at 600 °C (Figure S6), which aligns with previous reports.[52] cPLA and PLA-*g*-Cur05 displayed the lowest thermal stability, which could be attributed to radically induced PLA degradation resulting in low-molecular-weight oligomers. In contrast, PLA-*g*-Cur1 and PLA-*g*-Cur2 films displayed significantly higher decomposition temperatures than gPLA, suggesting that the increased curcumin concentrations not only inhibited PLA degradation during reactive extrusion but also introduced stabilizing effects beneficial to thermal processing. The ∼20 °C observed increase in decomposition temperatures ($T_{95}$ and $T_{50}$, the temperatures at which 5 and 50% of the mass was lost, respectively) could be attributed to the strong compatibilization between PLA chains through hydrogen bonding with curcumin, in agreement with prior reports on the thermal properties of polymers after blend compatibilization.[53] The observed increase may also be a result of the curcumin in the grafted polymer, affecting the thermodegradation occurring during TGA analysis. The enhanced thermal stability of PLA-*g*-Cur1 and PLA-*g*-Cur2 can have benefits in industry, particularly in processes involving high temperatures or long processing times. Additionally, in the presence of oxygen, these polymers may display even greater improvement in thermal stability due to curcumin's capacity to prevent thermal oxidation of the PLA by radical scavenging of ROS.[54]

DSC was used to quantify the thermal characteristics relevant for polymer processing and applications (Table 3). As a semicrystalline thermoplastic polymer, PLA exhibited glass transition ($T_g$), crystallization ($T_c$), and melting temperature ($T_m$). The results demonstrated no practical differences in thermal properties between treated and control films. However, we can evaluate the nuances of these results as a tool to better understand the effects of radical processing on polymer properties. The $T_m$ of cPLA was approximately 2 °C below that of PLA-*g*-Cur films and 4 °C below that of gPLA, likely due to the presence of low-molecular-weight oligomers created by chain scission during radical extrusion. Slight decreases in $T_m$ for PLA-*g*-Cur films compared to that for gPLA could be attributed to the disrupted stacking of polymer chains by the presence of curcumin. The largest differences in the DSC thermal properties are observed for the $T_c$ values of gPLA, cPLA, and PLA-*g*-Cur films. cPLA displayed the lowest $T_c$, which aligns with the DSC results of a previous work that reacted PLA with 0.5% w/w DCP.[47] The reduced $T_c$ of cPLA compared to that of gPLA could be attributed to branching and chain scission during processing, which results in the dispersity of oligomers, creating crystal defects and imperfect chain folding during crystallization. The 5−6 °C decrease in $T_c$ for PLA-*g*-Cur compared with that for gPLA could be a result of the reduced chain mobility from covalent immobilization of curcumin. Higher chain mobility decreases the energy required for polymer folding, which increases the temperature at which crystallization can occur.[55]

Overall, analysis of the thermal decomposition, melt, and crystallization behavior of the control (gPLA), process control (cPLA), and curcumin-grafted PLA (PLA-*g*-Cur) supports our hypothesis that curcumin reduces radical chain scission and cross-linking during the reactive extrusion of PLA, as demonstrated by the inferior thermal stability of cPLA. Similarly, poor thermal stability is observed in PLA-*g*-Cur05, likely due to the curcumin concentration being too low to significantly inhibit radical chain scission and cross-linking. The improvement in thermal stability (increased $T_{95}$ and $T_{50}$) when curcumin is increased in the feed from 0.5 to 1.0 and 2.0% w/w may indicate increased covalent grafting and antioxidant stabilization, which would mitigate chain scission and cross-linking. These results are demonstrative of why Irganox and other antioxidant stabilizers are used to prevent the deterioration of polymer properties during high-temperature processing.[14]

*Migration Assay in Food Simulants.* A migration assay based on EU and FDA recommendations for food contact materials was used to evaluate the extent of curcumin immobilization in functionalized films.[35,36] Food simulants used in the study included $H_2O$ (aqueous foods), 3% acetic acid (acidic foods), 10% EtOH (hydrophilic and low alcohol foods), and fractionated coconut MCT oil (fatty foods). PLA-*g*-Cur and gPLA were immersed in each food simulant for 10 days at 40 °C, and the concentration of migrated curcumin was determined spectrophotometrically (Table S2). For all food simulants, curcumin migration was below the limit of detection (0.000625 mg/cm$^2$) and exhibited no visible leaching (Figure S9). As the migratory limit established by the EU is 0.10 mg/cm$^2$, all PLA-*g*-Cur films are at least 160× below the migratory limit and can therefore be considered appropriate for the wide range of food applications simulated by this migration assay.

Polymer films extruded without the DCP radical initiator (PLA/Cur05, PLA/Cur1, and PLA/Cur2) were also evaluated in the migration assay to investigate the impact of radical grafting on curcumin immobilization. Interestingly, ungrafted films also demonstrated curcumin migration below the limit of detection and without visible leaching in all food simulants (Figure S9). The lack of curcumin migration in aqueous matrices ($H_2O$, 10% EtOH, and 3% acetic acid) may be expected due to curcumin's low water solubility. However, in coconut oil, curcumin has a reported solubility of up to 17.75 ± 2.40 mg/mL,[56] which would equate to a maximum of 88.75 mg/cm$^2$ in this study. Considering <0.000625 mg/cm$^2$ curcumin migration was observed in coconut oil, low migration results could not be attributed to solubility limits. Therefore, we hypothesize that noncovalent intermolecular interactions, such as hydrogen bonding between curcumin and PLA, immobilize curcumin within the polymer matrix.

*Curcumin Migration from Ungrafted Control Films during EtOH Incubation.* Migration studies validated the immobilization of curcumin in PLA-*g*-Cur films using EU and FDA regulatory standard methods, supporting the use of PLA-*g*-Cur materials in a wide range of packaging applications. However, due to the insignificant differences between PLA-*g*-Cur and PLA/Cur results, these studies did not demonstrate the importance of DCP in curcumin immobilization. Therefore, further assessment was conducted in harsher, nonfood simulant conditions to identify the differences in curcumin migration between covalently grafted and noncovalently blended films. It is important to note that these migration experiments serve the purpose of characterizing the materials rather than assessing their migration in real food packaging applications. Indeed, according to FDA guidelines, 95% EtOH


https://doi.org/10.1021/acsapm.3c01820
ACS Appl. Polym. Mater. 2024, 6, 192−206

is not a recommended food simulant due to its tendency to overexaggerate migration from food contact polymers (apart from polyolefins)[36] and was therefore not used as a simulant in the standard migration study for PLA-*g*-Cur films. Although 95% EtOH would be an inappropriate solvent for migratory studies simulating end use packaging applications, we used this solvent to characterize the covalency of curcumin immobilization during the reactive extrusion grafting. PLA-*g*-Cur and PLA/Cur films were incubated in 100% EtOH with constant shaking for 24 h. We expected that under these harsh incubation conditions, the strength of covalent bonds in PLA-*g*-Cur films would result in significantly less curcumin migration than from the PLA/Cur films. Aliquots were measured for curcumin concentration at select time points to observe the kinetics of migration from different films (Figure 1). For samples with the same curcumin concentration, films

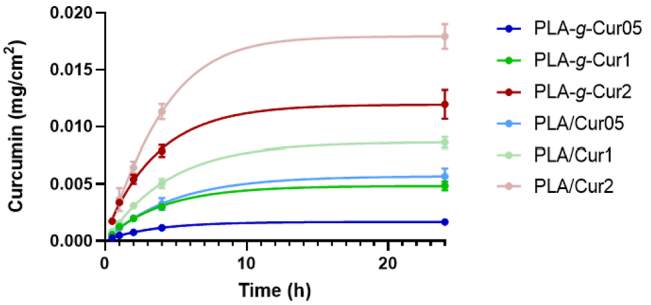


**Figure 1.** Curcumin migration from PLA-*g*-Cur films during shaking incubation in 100% EtOH. Data points were fit to a sigmoidal dose−response curve and signify the mean and standard deviation of six replicates for each time point.

processed with DCP demonstrated significantly less curcumin migration than films processed without DCP. Additionally, PLA/Cur films collectively demonstrated a faster release of curcumin at earlier points compared to PLA-*g*-Cur films (Figure S10). For example, PLA/Cur2 released nearly the same amount of curcumin in 4 h (0.0113 ± 0.0007 mg/cm$^2$) as PLA-*g*-Cur2 released in 24 h (0.0119 ± 0.0012 mg/cm$^2$). While all films would be considered below the EU migratory limit for aqueous, acidic, and fatty food applications based on results from the standard migration assay, this experiment demonstrates the improved stability of curcumin immobilization in radically grafted samples. Under harsh processing or storage conditions, it is advantageous to use packaging materials with reduced potential for leaching, which could cause defects in the color, taste, and texture of the product.

*UV−Visible Light Properties.* UV light can promote the photooxidation of food products, leading to off-odors, discoloration, and degradation of nutritional components.[57] Thus, it is beneficial for packaging materials to inhibit UV light transmission to food and beverages while maintaining a high visible light transmittance, which allows manufacturers and consumers to see packaged products. The UV-blocking and visible light transmittance of PLA-*g*-Cur films were evaluated by UV−vis spectrophotometry (Figure 2) based on previous studies demonstrating UV barrier properties of curcumin-based packaging.[58] According to the results, all PLA-*g*-Cur films demonstrated almost complete blocking in both the UV-B (280−315 nm) and UV-A (315−400 nm) region while conserving the optical transmittance of gPLA. The high optical transmittance of these films indicates good compatibility

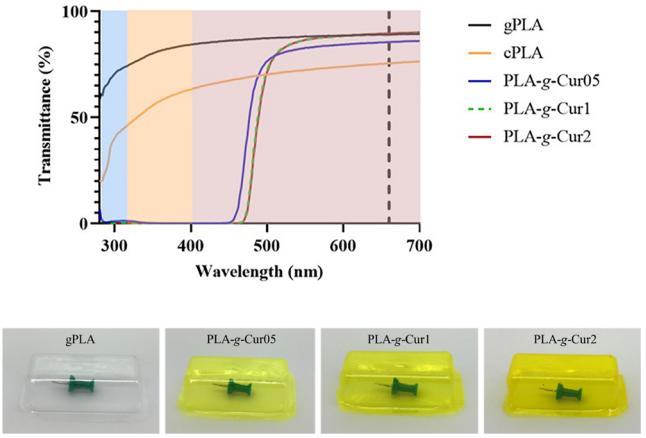


**Figure 2.** (Above) UV−vis spectra of PLA-*g*-Cur and control films to demonstrate UV-blocking and optical transmittance properties of treated samples. UV-B (280−315 nm), UV-A (315−400 nm), and visible (400−700 nm) regions are highlighted by blue, orange, and red shading, respectively. The 660 nm wavelength, which is used to determine the optical transmittance of a material, is signified by the dashed line. Curves are the average of eight replicates for each sample. For values outside the limit of detection for the UV−vis spectrophotometer, the highest absorption value among all samples ($A_{max}$ = 3.5) was used for calculations. (Below) thermoformed PLA-*g*-Cur material to demonstrate optical transmittance. Images were taken by a digital camera on a single representative sample, and a thumbtack was placed as a reference for transparency.

between curcumin and the PLA matrix.[59] The transparency of PLA-*g*-Cur films was visually demonstrated by thermoformed molds that exemplify how manufacturers and consumers could see products within PLA-*g*-Cur packaging (Figure 2).

The differences in transmittance between treated and control films were compared at 280 and 660 nm, which are the standard wavelengths to determine UV and optical transmittance, respectively (Table 4).[58,60] The reduced optical transmittance of cPLA could be attributed to the formation of short-chain oligomers and cross-linked polymer that reduces the crystallinity of the polymer matrix.[61] Mileva et al. reported the correlation between decreasing crystallization temperatures and increasing optical haze of polymers,[62] which aligns with the thermal and optical properties of cPLA. Additionally, low optical transmittance of cPLA supports our previously reported water contact angle data, since high hysteresis values have been associated with low polymer transparency.[63] In contrast to cPLA, PLA-*g*-Cur1 and PLA-*g*-Cur2 films retained complete optical transmittance of gPLA after reactive extrusion, suggesting that the presence of curcumin reduces the degradation of PLA that contributes to optical haze. In addition, all PLA-*g*-Cur films demonstrated >93.4% UV barrier properties, which could be utilized to prevent the oxidation of packaged products such as dairy, meat and seafood, and edible oils. These results validate the utility of curcumin immobilization in valorizing PLA packaging while minimizing the drawbacks associated with reactive extrusion of biodegradable polymers.

Characterization results for PLA-*g*-Cur and control films highlight the impact of curcumin on the physical performance of polymers processed by reactive extrusion. cPLA demonstrated the degradation of gPLA native properties during radical processing that leads to poor mechanical, thermal, and


https://doi.org/10.1021/acsapm.3c01820
ACS Appl. Polym. Mater. 2024, 6, 192−206

Table 4. UV ($T_{280}$) and Optical ($T_{660}$) Transmittance of PLA-*g*-Cur and Control Films to Quantitatively Determine Optical Properties[a]

| sample ID | gPLA | cPLA | PLA-*g*-Cur05 | PLA-*g*-Cur1 | PLA-*g*-Cur2 |
|---|---|---|---|---|---|
| $T_{280}$ (%) | 59.0 ± 9.3$^{A}$ | 21.7 ± 8.9$^{B}$ | <6.6$^{C}$ | <6.6$^{C}$ | <6.6$^{C}$ |
| $T_{660}$ (%) | 89.0 ± 2.4$^{AB}$ | 76.6 ± 13.5$^{A}$ | 85.6 ± 5.2$^{AB}$ | 89.1 ± 1.1$^{B}$ | 89.6 ± 1.6$^{B}$ |

[a]Values are the average and standard deviation of six replicate coupons for each treatment, and values outside the limit of detection for the UV−vis spectrophotometer are indicated. Letters signify statistically significant differences between samples for each wavelength (Tukey's HSD, $p \leq 0.05$).

optical performance. PLA-*g*-Cur05 displayed similar properties to those of cPLA, likely due to only partial inhibition of PLA degradation by curcumin during extrusion. On the other hand, PLA-*g*-Cur1 and PLA-*g*-Cur2 displayed curcumin immobilization in all food matrices while enhancing certain physical properties. These polymers exhibited significant improvement in thermal stability and nearly complete UV barrier properties while retaining the mechanical performance and optical transmittance of gPLA. Overall, these characterization results highlight the potential for replacing current PLA packaging systems with PLA-*g*-Cur without the risk of inferior optical, mechanical, or thermal properties and with the benefits of improved thermal stability and inhibition of photodegradation.

**Antioxidant and Color-Changing Performance of PLA-*g*-Cur Films.** *ABTS and DPPH Radical Scavenging Assays.* Antioxidants are a major class of preservative compounds directly added to food, primarily to inhibit radically induced lipid oxidation, which leads to deterioration of texture, flavor, odor, and nutritional value of products.[64] DPPH and ABTS radical scavenging assays were employed to measure the antioxidant capacity of the PLA-*g*-Cur films (Figure 3). DPPH is a standard method traditionally used to measure the radical scavenging activity of nonpolar and polyphenolic compounds by incubation in methanol (MeOH) or EtOH.[65] However, due to the exaggerated migration from nonpolyolefin polymers in 100% EtOH (as described previously), a 50% EtOH matrix was employed in this assay, which is an FDA-approved simulant for PLA.[36] PLA-*g*-Cur films were also evaluated by the ABTS standard method, which measures the radical scavenging activity of compounds for lipophilic and hydrophilic applications by incubation in pH-adjusted buffer. Standard curves of Trolox, a synthetic equivalent of vitamin E, were used to quantify the antioxidant performance of each sample.

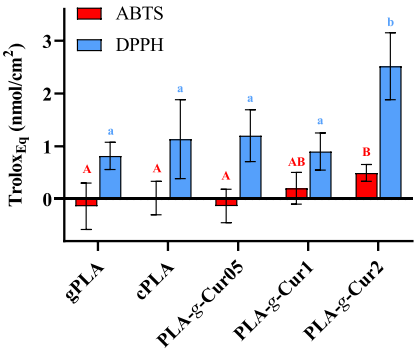


**Figure 3.** ABTS and DPPH radical scavenging assays to demonstrate the antioxidant capacity of PLA-*g*-Cur and control films. Quantification was performed by a Trolox standard curve, and the average value of quadruplicate blank samples (wells containing no films) were subtracted to obtain final values. Values denote the average and standard deviation of four replicates from each of two independently extruded batches, totaling eight replicates per treatment. Color-coded letters indicate statistically significant differences between sample means for each assay (Tukey's HSD, $p \leq 0.05$).

ABTS and DPPH assays demonstrated similar results with insignificant radical scavenging in all treated samples apart from PLA-*g*-Cur2. According to previous studies, curcumin primarily radical scavenges by two mechanisms: hydrogen atom transfer (HAT) from the phenolic moiety or sequential proton loss electron transfer (SPLET) from the keto-enol group. Under ionizing conditions, such as alkali buffers or EtOH, curcumin will radical scavenge by the SPLET mechanism: deprotonation at the keto-enol group and subsequent electron donation from the anion to the DPPH or ABTS radical. Under nonionizing conditions, such as neutral or acidic buffers, curcumin will not be deprotonated, resulting in radical scavenging by the HAT mechanism from the phenol.[20]

Previous research has demonstrated the significance of pH conditions on radical scavenging kinetics.[66,67] Therefore, it is worth noting that the ABTS assay performed in this work was executed at pH 7.4, which is below the p$K_a$ value of curcumin's enolic hydrogen (7.8).[68] Consequently, curcumin was not deprotonated under these assay conditions, suggesting that ABTS radical scavenging by PLA-*g*-Cur films was limited to the HAT mechanism. According to Litwinienko and Ingold, the HAT mechanism is significantly slower than the SPLET mechanism for curcumin,[20] indicating that the antioxidant capacity of PLA-*g*-Cur films may have been restricted by the time constraints of the assay. If the ABTS assay was performed at pH ≥ 7.8, we predict the SPLET mechanism would be favored and radical scavenging capacity would significantly increase. However, food systems are typically neutral or acidic in nature, and therefore, we chose not to exaggerate the radical scavenging capacity of PLA-*g*-Cur under nonapplicable conditions.

Our previous work involving polypropylene-*graft*-curcumin (PP-*g*-Cur) demonstrated significant DPPH radical scavenging capacity, up to 11.67 Trolox$_{Eq}$ (nmol/cm$^2$) for the 2% w/w curcumin sample (PP-*g*-Cur2).[31] In contrast, the PLA-*g*-Cur2 films analyzed in this DPPH assay demonstrated only 2.52 Trolox$_{Eq}$ (nmol/cm$^2$). While the differences between PLA and PP polymer matrices may have some effect on the radical scavenging capacities of these two films, the DPPH solvents may have a larger impact. Since PP-*g*-Cur is a polyolefin, the DPPH assay could be analyzed in 100% EtOH, as the incubation conditions were unlikely to exaggerate the migration of curcumin from the film. However, PLA-*g*-Cur samples needed to be analyzed in 50% EtOH, since 100% EtOH would force the leaching of curcumin from the PLA matrix. The 50% EtOH incubation solvent may have reduced ionizing potential compared to that of 100% EtOH, which could minimize the deprotonation of the keto-enol moiety of curcumin. As a result, while PP-*g*-Cur2 films could scavenge by the fast SPLET mechanism in 100% EtOH, PLA-*g*-Cur2 may


https://doi.org/10.1021/acsapm.3c01820
ACS Appl. Polym. Mater. 2024, 6, 192−206

be restricted to the slower HAT mechanism in 50% EtOH. The radical scavenging capacity of PLA-*g*-Cur was also evaluated by DPPH in 100% EtOH conditions; however, visibly leached curcumin led to significant exaggeration of the radical scavenging capacity (Figure S11). These results highlight the importance of assay conditions in the evaluation of a material's radical scavenging performance, as radical scavenging kinetics in different solvents can strongly influence the final results. In addition, it is important to design application-driven experiments to convey the true performance of technologies under commercially relevant conditions. For instance, while executing the DPPH assay in 100% EtOH would improve the antioxidant activity of PLA-*g*-Cur films reported in this study, instability of PLA in organic matrices renders these conditions irrelevant to the final application of PLA-*g*-Cur packaging. Overall, DPPH and ABTS assays demonstrate the modest potential of PLA-*g*-Cur films as radical scavenging packaging; however, further applications studies such as inhibition of oil oxidation would be invaluable in demonstrating their functionality in real food systems.

*Color Changing Response to Ammonia.* Intelligent packaging is an emerging technology that can indicate spoilage to the consumer or manufacturer through a colorimetric approach. Compared to traditional methods of determining spoilage such as bacterial plate count, colorimetric readings require less time and resources and can also be used at the household level to prevent spoilage-related illnesses for consumers. Several migratory intelligent packaging systems incorporating curcumin have demonstrated successful visual and quantitative indication of microbial growth in real food applications.[18,25] During meat and seafood storage, bacteria release TVBN gases that can deprotonate the phenol and keto-enol groups of curcumin, resulting in a color change that can be used to indicate product spoilage. The intelligent properties of PLA-*g*-Cur films were evaluated by the color change response to ammonia vapors, which simulate the TVBN released by spoilage bacteria. Results were collected visually with a digital camera and quantitatively with a colorimeter (Figure 4). $\Delta E^*$ indicates the total color change, and $\Delta C^*$ represents the change in the chromatic parameter, which excludes changes in lightness/darkness. This parameter was included to indicate that the majority of $\Delta E^*$ could be attributed to chromatic color change rather than darkening of the film. Compared to gPLA, all PLA-*g*-Cur films demonstrated practically significant visual and quantitative color change. PLA-*g*-Cur2 displayed the greatest color change response to ammonia; however, there was no significant difference between PLA-*g*-Cur05 and PLA-*g*-Cur1 color change. While it would be expected that increasing the curcumin concentration from 0.5 to 1.0% w/w would have an observable effect on color change, the similarity between the color changing properties of PLA-*g*-Cur05 and PLA-*g*-Cur1 is consistent with the water contact angle and radical scavenging results. Color change, water contact angle, and radical scavenging are all dependent on material interfacial properties; therefore, it is likely that the superior performance of PLA-*g*-Cur2 can be attributed to improved interfacial interactions with curcumin. A possible explanation is the orientation of grafted curcumin ligands toward the polymer matrix rather than the polymer/vapor interface due to hydrogen bonding with PLA. PLA-*g*-Cur2 may contain a higher concentration of surface-oriented curcumin due to oversaturation of PLA hydrogen bonding sites, resulting in improved performance in studies dependent on surface interaction.

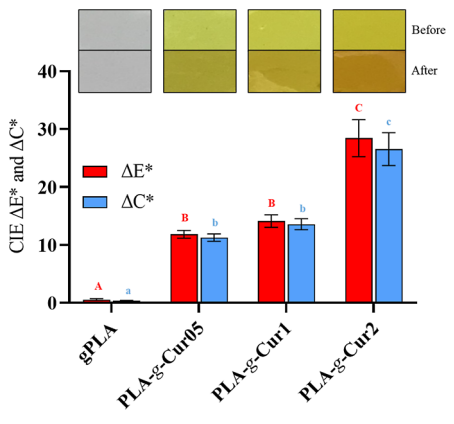


**Figure 4.** Color-changing properties of PLA-*g*-Cur films upon exposure to ammonia vapor. The chart indicates the total color change ($\Delta E^*$) and change in the chromatic parameter ($\Delta C^*$), and images are digital photographs of films taken in a light box before and after 24 h of ammonia exposure. Values are the mean and standard deviation of six replicates for each treatment. Color-coded letters signify significant differences between sample means for each of the measured parameters (Tukey's HSD, $p \leq 0.05$).

While these results indicate that PLA-*g*-Cur films can be used for intelligent packaging applications, the polymer system could be optimized for more identifiable color change. For instance, our previous work demonstrated that the $\Delta E^*$ value for PP-*g*-Cur2 films ($\Delta E^* \sim 50$) is nearly double that of PLA-*g*-Cur2 films ($\Delta E^* = 28$). Cvek et al. analyzed PLA/PPC films loaded with 2% w/w curcumin that had an ammonia response of $\Delta E^* \sim 70$.[24] If the exclusive purpose of developing these PLA-*g*-Cur films was for visible spoilage indication, then the films could be migratory since the indicators would be placed in the headspace of the packaging system. Consequently, to observe the greatest color change, we would create films containing the maximum curcumin concentration (while optimizing cost of inputs vs color-changing impact) and omit the DCP initiator. Additionally, a polymer matrix with minimal interaction with TVBN would be advantageous to optimize curcumin deprotonation under alkaline conditions. PLA contains carboxylic acid end groups with $pK_a \sim 3$, which, upon exposure to TVBN, will be deprotonated before curcumin.[69] Furthermore, a polyolefin with reduced compatibility with curcumin may improve color change by maximizing surface orientation toward the TVBN interface.

Overall, the results demonstrate modest intelligent properties of PLA-*g*-Cur films. Additionally, these results signify stability of curcumin during reactive extrusion since decomposition products such as ferulic acid and 4-vinyl guaiacol are incapable of such color change. While the color-changing properties of PLA-*g*-Cur films can provide value as spoilage indicators, intelligent packaging systems can be optimized through intentional design of the polymer structure and composition to enhance color change. These studies emphasize the value of applications-driven research to maximize the performance of functional materials under conditions of intended use.

*Color Changing Response to Shrimp Spoilage.* Finally, PLA-*g*-Cur films were evaluated for their ability to detect shrimp spoilage during storage at 4 °C. Based on the results of the ammonia study, only PLA-*g*-Cur2 was included in this


https://doi.org/10.1021/acsapm.3c01820
ACS Appl. Polym. Mater. 2024, 6, 192−206

experiment. Films were incubated in the headspace of shrimp storage jars, and the change in ΔC* of PLA-*g*-Cur2 was plotted against the TVC of shrimp (Figure 5). PLA-*g*-Cur2 films

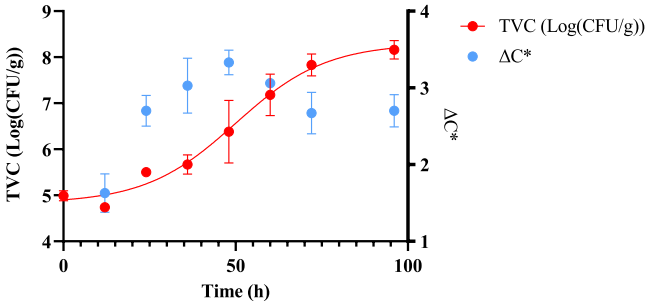


**Figure 5.** TVC of shrimp during spoilage at 4 °C with corresponding change in the chromatic parameter (ΔC*) of PLA-*g*-Cur films in the headspace of the storage jars. TVC data points are the average and standard deviation of triplicate shrimp, and colorimetric data points are the average and standard deviation of triplicate films.

appeared to change color significantly during the log phase of bacterial growth, reaching peak Δ*C** at the inflection point of the growth curve (48 h). However, as the rate of bacterial growth slowed, the Δ*C** values of the films decreased. A possible explanation for this pattern is the release of other volatile compounds during cell death (after log phase), such as acetic acid, lactic acid, or hydrogen sulfide that can neutralize the effect of TVBN on curcumin color change.[70] Compared with ammonia, the color change response of PLA-*g*-Cur2 to shrimp spoilage was significantly reduced. This work underscores the importance of using real food systems to evaluate the performance of materials, especially since the optimized and oversimplified conditions of standard methods can significantly overestimate the results.

## CONCLUSIONS

The aim of this research was to develop an active and intelligent biodegradable packaging system through the reactive extrusion of curcumin and PLA. Migration testing in accelerated storage conditions confirmed the immobilization of curcumin in PLA-*g*-Cur in aqueous, hydrophilic, acidic, and fatty food systems. Incubation in 100% EtOH supported that DCP radical grafting imparted covalent linkages between the curcumin and PLA backbone, improving the immobilization of the active ligand within the polymer matrix. However, it is worth noting that films extruded with DCP demonstrated a detectable degree of curcumin migration in 100% EtOH, indicating that some curcumin remained ungrafted in the PLA-*g*-Cur films. In future work, further optimization of extrusion conditions and reagent concentrations could improve the degree of grafting. However, the overall results demonstrate how DCP could be used to improve the immobilization of curcumin onto PLA compared to nonreactive blends. While curcumin is generally recognized as safe (GRAS) and poses limited toxicity concerns, the demonstrated success of radically grafting functional ligands onto thermoplastics offers a pathway to expand this technology to other active compounds with or without the GRAS status. Dynamic water contact angle, DSC thermal characterization, mechanical testing, and WVP studies demonstrated the conserved physical properties of gPLA in treated films. Additionally, all PLA-*g*-Cur films were capable of blocking >93.6% of UV light while retaining complete optical transmittance of PLA. Thus, PLA-*g*-Cur materials can inhibit the photooxidation of vitamins, minerals, proteins, and lipids in foods and beverages while allowing unobstructed visibility of the packaged product. The similar wettability, thermal, mechanical, water barrier, and optical properties of treated films suggest limited thermal degradation of PLA due to the stabilization effects of curcumin during reactive extrusion. These results are supported by the inferior thermal stability and optical transmittance of cPLA compared to those of PLA-*g*-Cur1 and PLA-*g*-Cur2 films, which can be attributed to cross-linking and chain scission reactions during extrusion that were not inhibited by the presence of an antioxidant stabilizer. Therefore, radical functionalization with curcumin is a strategy to enhance the optical properties and thermal stability of PLA materials while limiting the thermal degradation associated with reactive extrusion of biodegradable polyesters. Advanced analysis of possible byproduct production, impact on polymer molecular weight, and degree of functionalization during the radical-initiated grafting should be performed prior to commercial adoption of the material.

In regard to active and intelligent properties, PLA-*g*-Cur films displayed modest potential for radical scavenging and spoilage-indicating applications, more suitable for interpretation at the retail level with analytical color measurement than at the consumer level for visual interpretation. However, we hypothesize that the high compatibility between PLA and curcumin may have minimized the surface orientation of the active ligand, particularly for PLA-*g*-Cur05 and PLA-*g*-Cur1 films. Future studies should evaluate the antioxidant capacity of PLA-*g*-Cur packaging against lipid oxidation in real food systems, such as edible oil, meat, and seafood. Applications testing of PLA-*g*-Cur films would provide a better measure of radical scavenging capacity than standard assays that use pH and solvent conditions nonapplicable to food and beverage systems. Regarding intelligent properties, PLA-*g*-Cur2 films demonstrated significant color change in the presence of ammonia and modest color change in the presence of shrimp spoilage. These antioxidant and color changing assays demonstrate the importance of application-driven research to assess the performance of functional materials under commercially relevant conditions. For instance, while evaluating PLA-*g*-Cur films in standard DPPH organic solvent would result in significantly higher radical scavenging activity compared to the results reported in this work (Figure S11), 100% EtOH conditions are neither appropriate for PLA materials nor relevant to the conditions of intended use. Furthermore, the color change of PLA-*g*-Cur films under standard ammonia conditions signified excellent spoilage-indicating properties; however, real applications studies using conditions of packaged shrimp demonstrated a more modest performance.

Overall, these results demonstrate a scalable method to immobilize curcumin onto PLA for the production of active and intelligent UV-blocking packaging with improved thermal stability, thereby valorizing PLA beyond its traditional use in biodegradable packaging. This research advances the capabilities of functional materials through the establishment of methods to modify biodegradable polymers without the degradation of physical properties. Moreover, this work emphasizes how application-driven research can be used to tailor the properties of materials for conditions of intended use, improving both functional performance and potential for commercial translation.


https://doi.org/10.1021/acsapm.3c01820
ACS Appl. Polym. Mater. 2024, 6, 192−206

## ■ ASSOCIATED CONTENT

### Supporting Information

The Supporting Information is available free of charge at https://pubs.acs.org/doi/10.1021/acsapm.3c01820.

Raw dynamic water contact angle data for treated and control films; stress−strain curves from mechanical properties measurements; photos of the WVTR experimental setup; WVTR curves of mass loss over time; DSC thermograms; TGA overlaid thermograms; UV−vis spectral sweep to determine the maximum absorption wavelength of the curcumin solution; curcumin standard curves in various solvents; photos of migration vials after incubation at 40 °C for 10 days; and DPPH radical scavenging activity of films in 100% EtOH (PDF)

## ■ AUTHOR INFORMATION


### Corresponding Author

**Julie M. Goddard** − *Department of Food Science, 365 Stocking Hall, Cornell University, Ithaca, New York 14853, United States;* orcid.org/0000-0002-3644-0732; Email: goddard@cornell.edu

### Author

**Halle N. Redfearn** − *Department of Food Science, 365 Stocking Hall, Cornell University, Ithaca, New York 14853, United States;* orcid.org/0000-0002-6086-413X

Complete contact information is available at: https://pubs.acs.org/10.1021/acsapm.3c01820


### Author Contributions

H.R.: Conceptualization, data curation, formal analysis, investigation, methodology, project administration, supervision, validation, visualization, writing—original draft preparation, and writing—review and editing. Julie M. Goddard: Conceptualization, funding acquisition, project administration, supervision, and writing—review and editing.

### Notes

The authors declare no competing financial interest.

## ■ ACKNOWLEDGMENTS

This work was supported by award numbers 2019-68015-29230 and 2019-38420-28975 from the U.S. Department of Agriculture's National Institute of Food and Agriculture. This work made use of the Cornell Center for Materials Research Shared Facilities, which is supported through the NSF MRSEC program (DMR-1719875). The authors thank Cornell Statistical Consulting Unit for their assistance in the statistical experimental design.

## ■ REFERENCES


(1) Xue, L.; Liu, G.; Parfitt, J.; Liu, X.; Van Herpen, E.; Stenmarck, Å.; O'Connor, C.; Östergren, K.; Cheng, S. Missing Food, Missing Data? A Critical Review of Global Food Losses and Food Waste Data. *Environ. Sci. Technol.* **2017**, *51* (12), 6618−6633.

(2) Goddard, J. M.; Talbert, J. N.; Hotchkiss, J. H. Covalent Attachment of Lactase to Low-Density Polyethylene Films. *J. Food Sci.* **2007**, *72* (1), E036−E041.

(3) Environmental Protection Agency. Reducing Wasted Food & Packaging: A Guide for Food Services and Restaurants. 2014, https://www.epa.gov/sites/default/files/2015-08/documents/reducing_wasted_food_pkg_tool.pdf (accessed Sep 23, 2023).

(4) MacArthur, E. Beyond plastic waste. *Science* **2017**, *358* (6365), 843.

(5) Tawakkal, I. S. M. A.; Cran, M. J.; Miltz, J.; Bigger, S. W. A Review of Poly(Lactic Acid)-Based Materials for Antimicrobial Packaging. *J. Food Sci.* **2014**, *79* (8), R1477−R1490.

(6) Ncube, L. K.; Ude, A. U.; Ogunmuyiwa, E. N.; Zulkifli, R.; Beas, I. N. Environmental Impact of Food Packaging Materials: A Review of Contemporary Development from Conventional Plastics to Polylactic Acid Based Materials. *Materials (Basel)* **2020**, *13* (21), 4994.

(7) Moad, G. The synthesis of polyolefin graft copolymers by reactive extrusion. *Prog. Polym. Sci.* **1999**, *24* (1), 81−142.

(8) Novák, I.; Borsig, E.; Hrčková, L.; Fiedlerová, A.; Kleinová, A.; Pollák, V. Study of surface and adhesive properties of polypropylene grafted by maleic anhydride. *Polym. Eng. Sci.* **2007**, *47* (8), 1207−1212.

(9) Moad, G. Chemical modification of starch by reactive extrusion. *Prog. Polym. Sci.* **2011**, *36* (2), 218−237.

(10) Li, T.-T.; Cheng, S.-B.; Feng, L.-F.; Gu, X.-P.; Duan, J.-T.; Jiang, M.-Z.; Zhang, C.-L. A review on the free radical grafting of vinyl monomers onto polyethylene and polypropylene by reactive extrusion. *Chem. Eng. Sci.* **2023**, *278*, 118916.

(11) Przybysz-Romatowska, M.; Haponiuk, J.; Formela, K. Reactive extrusion of biodegradable aliphatic polyesters in the presence of free-radical-initiators: A review. *Polym. Degrad. Stab.* **2020**, *182*, 109383.

(12) Bednarek, M.; Borska, K.; Kubisa, P. New Polylactide-Based Materials by Chemical Crosslinking of PLA. *Polym. Rev.* **2021**, *61* (3), 493−519.

(13) Rigoussen, A.; Verge, P.; Raquez, J.-M.; Dubois, P. Natural Phenolic Antioxidants As a Source of Biocompatibilizers for Immiscible Polymer Blends. *ACS Sustain. Chem. Eng.* **2018**, *6* (10), 13349−13357.

(14) Amorin, N. S. Q. S.; Rosa, G.; Alves, J. F.; Gonçalves, S. P. C.; Franchetti, S. M. M.; Fechine, G. J. M. Study of thermodegradation and thermostabilization of poly(lactide acid) using subsequent extrusion cycles. *J. Appl. Polym. Sci.* **2014**, *131*(6)..

(15) Hernández-García, E.; Vargas, M.; Chiralt, A. Effect of active phenolic acids on properties of PLA-PHBV blend films. *Food Packag. Shelf Life* **2022**, *33*, 100894.

(16) Yahyaoui, M.; Gordobil, O.; Herrera Díaz, R.; Abderrabba, M.; Labidi, J. Development of novel antimicrobial films based on poly(lactic acid) and essential oils. *React. Funct. Polym.* **2016**, *109*, 1−8.

(17) Mohamad, N.; Mazlan, M. M.; Tawakkal, I. S. M. A.; Talib, R. A.; Kian, L. K.; Fouad, H.; Jawaid, M. Development of active agents filled polylactic acid films for food packaging application. *Int. J. Biol. Macromol.* **2020**, *163*, 1451−1457.

(18) Roy, S.; Priyadarshi, R.; Ezati, P.; Rhim, J.-W. Curcumin and its uses in active and smart food packaging applications - a comprehensive review. *Food Chem.* **2022**, *375*, 131885.

(19) Barzegar, A. The role of electron-transfer and H-atom donation on the superb antioxidant activity and free radical reaction of curcumin. *Food Chem.* **2012**, *135* (3), 1369−1376.

(20) Litwinienko, G.; Ingold, K. U. Abnormal solvent effects on hydrogen atom abstraction. 2. Resolution of the curcumin antioxidant controversy. The role of sequential proton loss electron transfer. *J. Org. Chem.* **2004**, *69* (18), 5888−5896.

(21) Ak, T.; Gülçin, İ. Antioxidant and radical scavenging properties of curcumin. *Chem.-Biol. Interact.* **2008**, *174* (1), 27−37.

(22) de Campos, S. S.; de Oliveira, A.; Moreira, T. F. M.; da Silva, T. B. V.; da Silva, M. V.; Pinto, J. A.; Bilck, A. P.; Gonçalves, O. H.; Fernandes, I. P.; Barreiro, M.-F.; Yamashita, F.; Valderrama, P.; Shirai, M. A.; Leimann, F. V. TPCS/PBAT blown extruded films added with curcumin as a technological approach for active packaging materials. *Food Packag. Shelf Life* **2019**, *22*, 100424.

(23) Shen, W.; Yan, M.; Wu, S.; Ge, X.; Liu, S.; Du, Y.; Zheng, Y.; Wu, L.; Zhang, Y.; Mao, Y. Chitosan nanoparticles embedded with curcumin and its application in pork antioxidant edible coating. *Int. J. Biol. Macromol.* **2022**, *204*, 410−418.

(24) Cvek, M.; Paul, U. C.; Zia, J.; Mancini, G.; Sedlarik, V.; Athanassiou, A. Biodegradable Films of PLA/PPC and Curcumin as Packaging Materials and Smart Indicators of Food Spoilage. *ACS Appl. Mater. Interfaces* **2022**, *14* (12), 14654−14667.
(25) Yildiz, E.; Sumnu, G.; Kahyaoglu, L. N. Monitoring freshness of chicken breast by using natural halochromic curcumin loaded chitosan/PEO nanofibers as an intelligent package. *Int. J. Biol. Macromol.* **2021**, *170*, 437−446.
(26) Liu, J.; Wang, H.; Wang, P.; Guo, M.; Jiang, S.; Li, X.; Jiang, S. Films based on κ-carrageenan incorporated with curcumin for freshness monitoring. *Food Hydrocolloids* **2018**, *83*, 134−142.
(27) Maharana, T.; Pattanaik, S.; Routaray, A.; Nath, N.; Sutar, A. K. Synthesis and characterization of poly(lactic acid) based graft copolymers. *React. Funct. Polym.* **2015**, *93*, 47−67.
(28) Curcio, M.; Puoci, F.; Iemma, F.; Parisi, O. I.; Cirillo, G.; Spizzirri, U. G.; Picci, N. Covalent Insertion of Antioxidant Molecules on Chitosan by a Free Radical Grafting Procedure. *J. Agric. Food Chem.* **2009**, *57* (13), 5933−5938.
(29) Uyama, H.; Maruichi, N.; Tonami, H.; Kobayashi, S. Peroxidase-Catalyzed Oxidative Polymerization of Bisphenols. *Biomacromolecules* **2002**, *3* (1), 187−193.
(30) Herskovitz, J. E.; Goddard, J. M. Reactive Extrusion of Nonmigratory Antioxidant Poly(lactic acid) Packaging. *J. Agric. Food Chem.* **2020**, *68* (7), 2164−2173.
(31) Redfearn, H. N.; Warren, M. K.; Goddard, J. M. Reactive Extrusion of Nonmigratory Active and Intelligent Packaging. *ACS Appl. Mater. Interfaces* **2023**, *15* (24), 29511−29524.
(32) American Society for Testing and Materials. Standard Test Method for Tensile Properties of Thin Plastic Sheeting1 West Conshohocken: ASTM International. 2018, https://compass.astm.org/document/?contentCode=ASTM%7CD0882-18%7CEN-US&proxycl=https%3A%2F%2Fsecure.astm.org&fromLogin=true (accessed July 05, 2023).
(33) ASTM. ASTM E96/E96M-16: Standard Test Methodsfor Water Vapor Transmission of Materials West Conshohocken, PA: ASTMInternational; 2016. [Accessed July 05,2023]. Available from: https://www.astm.org/e0096_e0096m-16.html.
(34) Rhim, J.-W.; Hong, S.-I.; Ha, C.-S. Tensile, water vapor barrier and antimicrobial properties of PLA/nanoclay composite films. *LWT−Food Sci. Technol.* **2009**, *42* (2), 612−617.
(35) European Union. *Commission Regulation (EU) No 10/20/2011 on plastic materials and articles intended to come into contact with food: Official Journal of the European Union*, 2011; Vol. *045*, pp 42−130.
(36) Food and Drug Administration. Guidance for Industry: Preparation of Premarket Submissions for Food Contact Substances (Chemistry Recommendations). 2018, https://www.fda.gov/regulatory-information/search-fda-guidance-documents/guidance-industry-preparation-premarket-submissions-food-contact-substances-chemistry#ai (accessed Jan 13, 2022).
(37) Priyadarsini, K. I.; Maity, D. K.; Naik, G. H.; Kumar, M. S.; Unnikrishnan, M. K.; Satav, J. G.; Mohan, H. Role of phenolic O-H and methylene hydrogen on the free radical reactions and antioxidant activity of curcumin. *Free Radical Biol. Med.* **2003**, *35* (5), 475−484.
(38) Esatbeyoglu, T.; Ulbrich, K.; Rehberg, C.; Rohn, S.; Rimbach, G. Thermal stability, antioxidant, and anti-inflammatory activity of curcumin and its degradation product 4-vinyl guaiacol. *Food Funct.* **2015**, *6* (3), 887−893.
(39) Roy, S.; Rhim, J.-W. Preparation of bioactive functional poly(lactic acid)/curcumin composite film for food packaging application. *Int. J. Biol. Macromol.* **2020**, *162*, 1780−1789.
(40) Gong, J.; Tian, N.; Wen, X.; Chen, X.; Liu, J.; Jiang, Z.; Mijowska, E.; Tang, T. Synergistic effect of fumed silica with Ni2O3 on improving flame retardancy of poly(lactic acid). *Polym. Degrad. Stab.* **2014**, *104*, 18−27.
(41) Fijoł, N.; Abdelhamid, H. N.; Pillai, B.; Hall, S. A.; Thomas, N.; Mathew, A. P. 3D-printed monolithic biofilters based on a polylactic acid (PLA) − hydroxyapatite (HAp) composite for heavy metal removal from an aqueous medium. *RSC Adv.* **2021**, *11* (51), 32408−32418.
(42) Manju, P.; Krishnan, P. S. G.; Nayak, S. K. In situ polymerised PLA-SEP bionanocomposites: effect of silanol groups on the properties of PLA. *J. Polym. Res.* **2020**, *27* (5), 134.
(43) Hettiarachchi, S. S.; Dunuweera, S. P.; Dunuweera, A. N.; Rajapakse, R. M. G. Synthesis of Curcumin Nanoparticles from Raw Turmeric Rhizome. *ACS Omega* **2021**, *6* (12), 8246−8252.
(44) Zografi, G.; Johnson, B. A. Effects of surface roughness on advancing and receding contact angles. *Int. J. Pharm.* **1984**, *22* (2−3), 159−176.
(45) Carlson, D.; Dubois, P.; Nie, L.; Narayan, R. Free radical branching of polylactide by reactive extrusion. *Polym. Eng. Sci.* **1998**, *38* (2), 311−321.
(46) Extrand, C. W.; Kumagai, Y. An Experimental Study of Contact Angle Hysteresis. *J. Colloid Interface Sci.* **1997**, *191* (2), 378−383.
(47) Huang, Y.; Zhang, C.; Pan, Y.; Wang, W.; Jiang, L.; Dan, Y. Study on the Effect of Dicumyl Peroxide on Structure and Properties of Poly(Lactic Acid)/Natural Rubber Blend. *J. Polym. Environ.* **2013**, *21* (2), 375−387.
(48) Ren, Z.; Li, H.; Sun, X.; Yan, S.; Yang, Y. Fabrication of High Toughness Poly(lactic acid) by Combining Plasticization with Crosslinking Reaction. *Ind. Eng. Chem. Res.* **2012**, *51* (21), 7273−7278.
(49) Mooninta, S.; Poompradub, S.; Prasassarakich, P. Packaging Film of PP/LDPE/PLA/Clay Composite: Physical, Barrier and Degradable Properties. *J. Polym. Environ.* **2020**, *28* (12), 3116−3128.
(50) Marra, A.; Silvestre, C.; Duraccio, D.; Cimmino, S. Polylactic acid/zinc oxide biocomposite films for food packaging application. *Int. J. Biol. Macromol.* **2016**, *88*, 254−262.
(51) Tanetrungroj, Y.; Prachayawarakorn, J. Effect of dual modification on properties of biodegradable crosslinked-oxidized starch and oxidized-crosslinked starch films. *Int. J. Biol. Macromol.* **2018**, *120*, 1240−1246.
(52) Jafari, Y.; Sabahi, H.; Rahaie, M. Stability and loading properties of curcumin encapsulated in Chlorella vulgaris. *Food Chem.* **2016**, *211*, 700−706.
(53) Tomić, N. Z. Chapter 17—Thermal studies of compatibilized polymer blends. *Compatibilization of Polymer Blends*; Ajitha, A. R., Thomas, S., Ed.; Elsevier, 2020; pp 489−510.
(54) Yao, Z.; Gong, W.; Li, C.; Deng, Z.; Jin, Y.; Meng, X. Sustained antioxidant properties of epigallocatechin gallate loaded halloysite for PLA as potentially durable materials. *J. Appl. Polym. Sci.* **2023**, *140* (5), No. e53411.
(55) Li, H.; Huneault, M. A. Effect of nucleation and plasticization on the crystallization of poly(lactic acid). *Polymer* **2007**, *48* (23), 6855−6866.
(56) Patil, V.; Mhamane, S.; More, S.; Pawar, A.; Arulmozhi, S. Exploring the protective effect exhibited by curcumin-loaded coconut oil microemulsion in the experimental models of neurodegeneration: an insight of formulation development, in vitro and in vivo study. *Futur. J. Pharm. Sci.* **2022**, *8* (1), 51.
(57) Guzman-Puyol, S.; Hierrezuelo, J.; Benítez, J. J.; Tedeschi, G.; Porras-Vázquez, J. M.; Heredia, A.; Athanassiou, A.; Romero, D.; Heredia-Guerrero, J. A. Transparent, UV-blocking, and high barrier cellulose-based bioplastics with naringin as active food packaging materials. *Int. J. Biol. Macromol.* **2022**, *209*, 1985−1994.
(58) Roy, S.; Rhim, J.-W. Carboxymethyl cellulose-based antioxidant and antimicrobial active packaging film incorporated with curcumin and zinc oxide. *Int. J. Biol. Macromol.* **2020**, *148*, 666−676.
(59) Zhang, W.; Gui, Z.; Lu, C.; Cheng, S.; Cai, D.; Gao, Y. Improving transparency of incompatible polymer blends by reactive compatibilization. *Mater. Lett.* **2013**, *92*, 68−70.
(60) Rhim, J.-W.; Hong, S.-I.; Park, H.-M.; Ng, P. K. W. Preparation and Characterization of Chitosan-Based Nanocomposite Films with Antimicrobial Activity. *J. Agric. Food Chem.* **2006**, *54* (16), 5814−5822.
(61) Kim, H. H.; Song, D. W.; Kim, M. J.; Ryu, S. J.; Um, I. C.; Ki, C. S.; Park, Y. H. Effect of silk fibroin molecular weight on physical property of silk hydrogel. *Polymer* **2016**, *90*, 26−33.

(62) Mileva, D.; Tranchida, D.; Gahleitner, M. Designing polymer crystallinity: An industrial perspective. *Polym. Cryst.* **2018**, *1* (2), No. e10009.
(63) Larena, A.; Millán, F.; Pérez, G.; Pinto, G. Effect of surface roughness on the optical properties of multilayer polymer films. *Appl. Surf. Sci.* **2002**, *187* (3−4), 339−346.
(64) Alamed, J.; Chaiyasit, W.; McClements, D. J.; Decker, E. A. Relationships between Free Radical Scavenging and Antioxidant Activity in Foods. *J. Agric. Food Chem.* **2009**, *57* (7), 2969−2976.
(65) Nenadis, N.; Wang, L.-F.; Tsimidou, M.; Zhang, H.-Y. Estimation of Scavenging Activity of Phenolic Compounds Using the ABTS•+ Assay. *J. Agric. Food Chem.* **2004**, *52* (15), 4669−4674.
(66) Redfearn, H. N.; Goddard, J. M. Antioxidant and dissociation behavior of polypropylene-graft-maleic anhydride. *J. Appl. Polym. Sci.* **2022**, *139* (32), No. e52764.
(67) Ozgen, M.; Reese, R. N.; Tulio, A. Z.; Scheerens, J. C.; Miller, A. R. Modified 2,2-Azino-bis-3-ethylbenzothiazoline-6-sulfonic Acid (ABTS) Method to Measure Antioxidant Capacity of Selected Small Fruits and Comparison to Ferric Reducing Antioxidant Power (FRAP) and 2,2′-Diphenyl-1-picrylhydrazyl (DPPH) Methods. *J. Agric. Food Chem.* **2006**, *54* (4), 1151−1157.
(68) Zebib, B.; Mouloungui, Z.; Noirot, V. Stabilization of curcumin by complexation with divalent cations in glycerol/water system. *Bioinorg. Chem. Appl.* **2010**, *2010*, 292760.
(69) Siparsky, G. L.; Voorhees, K. J.; Miao, F. Hydrolysis of Polylactic Acid (PLA) and Polycaprolactone (PCL) in Aqueous Acetonitrile Solutions: Autocatalysis. *J. Environ. Polym. Degrad.* **1998**, *6* (1), 31−41.
(70) Li, X.; Zhu, J.; Li, C.; Ye, H.; Wang, Z.; Wu, X.; Xu, B. Evolution of Volatile Compounds and Spoilage Bacteria in Smoked Bacon during Refrigeration Using an E-Nose and GC-MS Combined with Partial Least Squares Regression. *Molecules* **2018**, *23* (12), 3286.


https://doi.org/10.1021/acsapm.3c01820
*ACS Appl. Polym. Mater.* 2024, 6, 192−206